Characterization of metal hydrides for thermal applications in vehicles below 0 °C

Mila Kölbig*, Inga Bürger, Marc Linder

German Aerospace Center (DLR), Institute of Engineering Thermodynamics, Thermal Process Technology, Pfaffenwaldring 38-40, 70569 Stuttgart, Germany

* Corresponding author: mila.koelbig@dlr.de, mila.dieterich@dlr.de; née Dieterich

Abstract

Metal hydrides promise great potential for thermal applications in vehicles due to their fast reaction rates even at low temperature. However, almost no detailed data is known in literature about thermochemical equilibria and reaction rates of metal hydrides below 0 °C, which, though, is crucial for the low working temperature levels in vehicle applications.

Therefore, this work presents a precise experimental set-up to measure characteristics of metal hydrides in the temperature range of -30 to 200 °C and a pressure range of 0.1 mbar to 100 bar. $LaNi_{4.85}Al_{0.15}$ and Hydralloy C5 were characterized. The first pressure concentration-isotherms for both materials below 0 °C are published. $LaNi_{4.85}Al_{0.15}$ shows an equilibrium pressure down to 55 mbar for desorption and 120 mbar for absorption at mid-plateau and -20 °C. C5 reacts between 580 mbar for desorption and 1.6 bar for absorption at -30 °C at mid-plateau.

For $LaNi_{4.85}Al_{0.15}$, additionally reaction rate coefficients down to -20 °C were measured and compared to values of $LaNi_5$ for the effect of Al-substitution. The reaction rate coefficient of $LaNi_{4.85}Al_{0.15}$ at -20 °C is 0.0018 s^{-1}. The obtained data is

discussed against the background of preheating applications in fuel cell and conventional vehicles.

Keywords

Metal hydride; pressure concentration-isotherm; reaction rate coefficient; $LaNi_{4.85}Al_{0.15}$; Hydralloy C5

Abbreviations

A	pre-exponential factor	s^{-1}
d	diameter	mm
E_a	activation energy	kJ/mol
eq	equilibrium	
f	factor between end and equilibrium pressure	
f(p)	pressure dependence function	
f(x)	reaction mechanism function	
FC	fuel cell	
H2	hydrogen	
(Hydralloy) C5	investigated material (for hydrogen supply) ($Ti_{0.95}Zr_{0.05}Mn_{1.46}V_{0.45}Fe_{0.09}$)	
ICE	internal combustion engine	
k	rate coefficient	s^{-1}
$LaNi_{4.85}Al_{0.15}$	investigated material (for preheating)	
m	mass	g
MH	metal hydride	
m_{pl}	plateau slope of PCI	wt.-%$^{-1}$
NPDM	normalized pressure dependence method [1]	
P	pressure	bar
PCI	pressure concentration-isotherm	
PEMFC	proton exchange membrane fuel cell	
R	gas constant, R = 8.314 J/(mol K)	J/(mol K)
S	Sieverts' volume	l
T	temperature	°C
t	time	s
tr	tube right	
V	volume	L
$\dot{V}$	volume flow	ml_N/min
VFC	volume flow control	
x	hydrogen conversion	
$\Delta_R H$	reaction enthalpy	kJ/mol
$\Delta_R S$	reaction entropy	J/(mol K)
ω	hydrogen conversion	wt.-%

1. Introduction

Cold start is a severe problem for vehicle drives such as internal combustion engines (ICE) or fuel cells (FC).

The challenge for ICEs are the emissions at low temperatures until the designated temperature of around 100 °C is reached. During the cold start phase neither the combustion process nor the exhaust gas treatment work sufficiently. Due to wall quenching in the cylinder and low combustion temperatures, the amount of pollutants is increased. Therefore, in these first couple of minutes, a great portion of all pollutants of the whole ride are produced. E.g. Cipollone et. al [2] state that around 60 % of harmful substances are produced during cold start. Even up to 80 % of some pollutant species are associated with cold start according to Reiter and Kockelman [3]. Cold start emissions include mainly nitrogen oxides, hydrocarbons (CH_4 and other HC) and volatile organic compounds. Faster heat-up would reduce the emissions drastically. [4]–[9]

Fuel cells face the challenge of degradation at temperatures below freezing point. If a proton exchange membrane fuel cell (PEMFC) is operated below 0 °C, the produced water might freeze and form an ice layer, which prevents gas flow and the expansion in volume can cause mechanical stress that leads to an shortened life time of the fuel cell. An application in vehicles therefore requires water management at low temperatures. Today, one state of the art start-up enhancement uses a positive temperature coefficient (PTC) heater run by electrical energy, which is itself very valuable at low temperatures and additionally might reduce the driving range. Preheating using surplus energy would increase the efficiency substantially. [10]–[13]

In both cases, waste heat at operation temperature level is available later on in the driving cycle. This time shift is the point of application considered in this work. With the help of thermal energy storage, the surplus energy can be made available for preheating at cold start. This way, besides emission reduction and efficiency increase, the component operation life could be prolonged.

The challenge is the usage of low level waste heat in a small storage able to provide heat within seconds or few minutes. The thermochemical reaction of metal hydrides with hydrogen has the potential to meet these requirements. Metal hydrides are metal alloys reacting exo-/endothermally with hydrogen according to equation (1) [14]. Besides storage applications, they receive increasing attention for thermal applications due to their very fast reaction, even at low temperatures.

$$MH_x + \frac{y}{2} H_2 \leftrightarrows MH_{x+y} + \Delta_R H \quad (1)$$

One important characteristic is the separation of hydrogen and the metal hydride, e.g. by a valve. This prevents the reverse reaction and the thermal energy can be stored as long as desired. The recombination generates heat and leads to a temperature increase of the solid material. Therefore, the storage can cool down to ambient temperature with no insulation required and generate the heat when needed. Another great advantage to sensible or phase change thermal storage is energy generation on demand and the higher energy density at a given temperature level.

In order to use metal hydrides for vehicle preheating, two characteristics of the reaction have to be known: the thermochemical equilibrium according to thermodynamics as well as the reaction rate that is dominated by intrinsic material properties. These terms are specified in the following.

The absorption of hydrogen in metal hydrides forms different phases. During the transition from α to the β-phase (called α+β-phase), much hydrogen can be absorbed by the solid metal leading to a comparatively low increase of the associated equilibrium pressure. This plateau represents the region which can be used most readily for metal hydride applications. This characteristic is described by pressure concentration-isotherms (PCIs). The pressure increases with increasing hydrogen conversion ($\omega = \frac{m_{H2}}{m_{MH}} \cdot 100$). Real metal hydrides show a hysteresis between absorption and desorption. From these PCIs, the plateau region is used to describe the equilibrium between gas pressure and metal hydride temperature in a van't Hoff-plot.

The overall reaction rate is influenced by the reaction mechanism, the materials' rate coefficient as well as by the distance to the thermodynamic equilibrium. Besides valid descriptions of these influences, precise measurements allowing unimpeded gas flow and optimal heat transfer for almost isothermal conditions are essential to the determination of the reaction rate. Details on the reaction mechanism are given e.g. in [15], [16]. Due to the very fast reaction of the materials considered here, precise measurements require a mature concept for the reactor and the experimental conditions. Details about the approach in this paper are given in the experimental section.

Two operation designs - an open system with single reaction in FC vehicles and a closed system with coupled reactions in ICEs – can be considered, as presented and discussed in [17], [18].

Since the reaction partner of metal hydrides is hydrogen, a metal hydride preheater for a FC vehicle consists of one reactor containing the heat generating material and

can be directly integrated into the hydrogen infrastructure. Hydrogen is supplied for preheating from the vehicle's hydrogen tank and desorbed by waste heat during regeneration and converted into electricity in the FC. Hence, no hydrogen is consumed. Such a system is considered **open** and reacts in a single reaction of the heat generating material.

An ICE vehicle doesn't have a hydrogen infrastructure. Hence, the hydrogen has to be supplied by another hydrogen supplying metal hydride in a second reactor. During discharge, the hydrogen supplying material desorbs hydrogen at a higher equilibrium pressure leading to an immediate absorption by the heat generating material. Waste heat during regeneration leads to a higher equilibrium pressure of the heat generating material and consequently recharges the hydrogen supplying material. This system is **closed** and consists of two strongly interdepended, coupled reactions of two different metal hydrides exchanging hydrogen.

The chosen materials are $LaNi_{4.85}Al_{0.15}$ as heat generating material and Hydralloy C5[a] ($Ti_{0.95}Zr_{0.05}Mn_{1.46}V_{0.45}Fe_{0.09}$) as hydrogen supplying material for the coupled reactions in the closed system. The latter was also used by Weckerle et. al [19] for high thermal power air conditioning. Based on extrapolation of so far known PCI data to lower temperature, the materials should fit well the restricting boundary conditions of the preheating application at winter temperatures between -20 and 20 °C. Waste heat levels are considered to be between 90 and 130 °C for ICEs (closed system) and 60 °C for FCs (open system). The pressure level was limited to 30 bar due to mechanical stresses on potential reactor designs.

[a] Hydralloy C-materials are AB_2 type hydride alloys numbered according to their percentage of other A-components than titanium. Therefore, $Ti_{0.95}Zr_{0.05}Mn_{1.46}V_{0.45}Fe_{0.09}$ – the material used in this study – is called Hydralloy C5® and is referred to as 'C5' in this work

The knowledge of the thermochemical equilibrium and the reaction of the considered materials is crucial in order to predict the potential of the thermal power output in particular of the coupled reactions, understand the reactions responds and identify relevant influencing factors on both the reaction itself and design parameters for the system. However, little is known about the material properties of metal hydrides below 0 °C in general and almost nothing has been published for the selected materials.

Regarding the thermodynamic properties of $LaNi_{4.85}Al_{0.15}$, only five publications could be found on pressure concentration-isotherms in a temperature range between 25 and 110 °C [20]–[24]. This is also true for C5, for which only few publications in a temperature range between 0 and 100 °C are available [25]–[27]. The data is shown in a van't Hoff plot in Figure 1, left, including in grey the range of interest for the presented application. A similar picture arises for kinetic properties. For $LaNi_{4.85}Al_{0.15}$, very little data exists [22], [28]. Furthermore, the investigated temperature levels are far above the range considered here and little information about the experiments and isothermal conditions is provided. More over even different equations have been used to derive the reaction rate. Therefore, this data can't be used for predictions of the material behavior down to -20°C. In order to narrow the range for the characteristics of $LaNi_{4.85}Al_{0.15}$, literature data of a comparable alloy, $LaNi_5$, is also considered. However, the effect of aluminum substitution on the reaction rate is discussed controversy in literature. Whereas some authors state a decreasing effect on the intrinsic kinetics, such as [29]–[31], others suggest an increasing effect, e.g. [22], [28], [32], [33]. The results of this work will be discussed against this background.

For C5, only one single publication could be found on kinetic investigations. The work of Skripnyuk and Ron [27] presented results down to a temperature of -20 °C and is used as a reference in this work. All kinetic data available is given Figure 1, right.

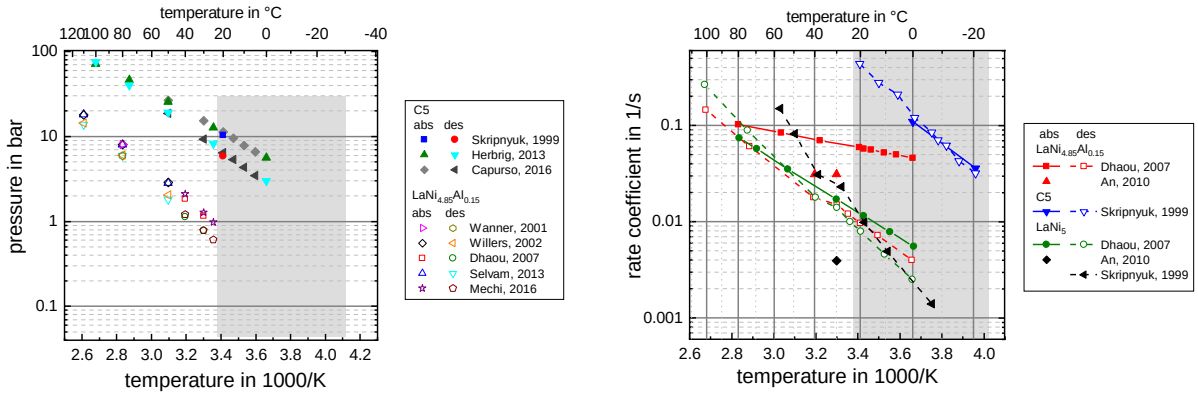

Figure 1. Available thermodynamic (left) [20]–[27] **and kinetic data (right)** [22], [27], [28] **for $LaNi_{4.85}Al_{0.15}$ and C5**

As can be seen from this literature review, no data on the thermodynamic equilibrium below 0 °C exists for both materials and no reliable kinetic data for $LaNi_{4.85}Al_{0.15}$ can be used. However, as this is crucial for the preheating application in vehicles, this data is obtained in this work.

For this purpose a precise experimental set-up is developed. Great care was taken to realize high precision and to exclude measurement errors and impacts of reactor or experimental design. Pressure concentration-isotherms (PCIs) are measured in a temperature range between -30 and 130 °C for both materials and reaction rate coefficients in the range between -20 and 40 °C are obtained for $LaNi_{4.85}Al_{0.15}$. Finally, the data is discussed regarding the suitability of the materials for the considered preheating application in vehicles.

2. Experimental

This section provides details about the methods of characterization, the test bench and the reactors as well as the analysis and the experimental design.

2.1.Method

PCI measurements require experiments very close to equilibrium. They can be measured either statically or dynamically.

The static measurement provides hydrogen to the material and allows sufficient time to reach equilibrium at the set temperature. Theses measurement steps are repeated several times, each step leading to one point of the PCI, until full conversion is reached. This type of measurement was performed extensively in literature, see e.g. [20], [26], [31], [34], [35]. Usually, little information is given about the testing procedure, such as the amount and pressure of hydrogen added or the resulting temperature peak inside the material. This, however, might influence the results, as mentioned by Friedlmeier et. al [36].

The dynamic method is rarely used in literature, e.g. by Muthukumar et. al [37]. During a dynamic measurement, hydrogen is supplied continuously resulting in continuous measurement values for the PCI. However, for such a measurement, the equilibrium state is disturbed at any time so the experimental variables have to be chosen with care [36]. This requires a considerable effort for the reactor design and experiment parameters. The heat management of the reactor has to be sufficient in order to ensure almost isothermal conditions and, thus, relate the results to the intended set temperature. The experiment has to be performed at such low hydrogen flow rates, that the material remains very close to equilibrium during reaction. If the flow rate is too high, the measurement is controlled by heat transfer rather than by

the equilibrium of the reaction. This leads to pressure values presumably too high or low for absorption and desorption, respectively. Therefore, the mass flow and temperature change have to be examined intensively to ensure appropriate measurements.

This work uses the dynamic method. To ensure accurate results, the equilibrium state and (almost) isothermal conditions are considered carefully and the results are compared to literature values at available temperatures.

The measurement procedure to determine the reaction rate coefficient has to exclude limitations of the reaction other than the kinetics in order to yield correct results. In particular for the fast reaction rates of the materials considered in this work, careful considerations have to ensure correct measurements. If in particular heat flow limitations are underestimated, reported results can divergent greatly, as discussed e.g. by Goodell and Rudman [38]. The normalized pressure dependence method (NPDM) suggested by Ron [1] is used to determine the kinetic values. The following conditions are suggested there:

- Temperature change of the material should be limited to ± 1 K, e.g. by the thermal ballast method
- Mass transfer of hydrogen through the reaction bed should be high so the gas transport does not limit the reaction
- A reaction order or mechanism must be defined
- Within the considered temperature range, the reaction process has to obey the Arrhenius temperature dependence
- The hydrogen should be converted within the plateau region (α+β region)

The restriction on the maximal temperature change is strict compared to other work. Rudman [39], for example, discusses a temperature change of ± 10 K. In order to be

able to refer the derived rate coefficient to one temperature, the maximal temperature change allowed in this work is ± 3 K.

2.2.Test bench and reactor design

A test bench was designed and brought into operation as shown in Figure 2. The left hand side depicts the layout of the bench with several hydrogen reservoirs (Sieverts' volumes, S1-S3) for flexible measurement of different probe masses. The range of the volume flow control (VFC) is small (0.5 … 25 ml_N/min) to allow the approach of the equilibrium state during PCI measurements. A bypass (V_{tr2} and V_{tr3}) allows fast pressure change for measurements of the kinetic rate coefficient. The temperature of the material is set by a thermostatic bath (-30 … 200 °C).

More details on the measurement equipment and accuracy are given in the supplementary material in Table A-1 and in [18].

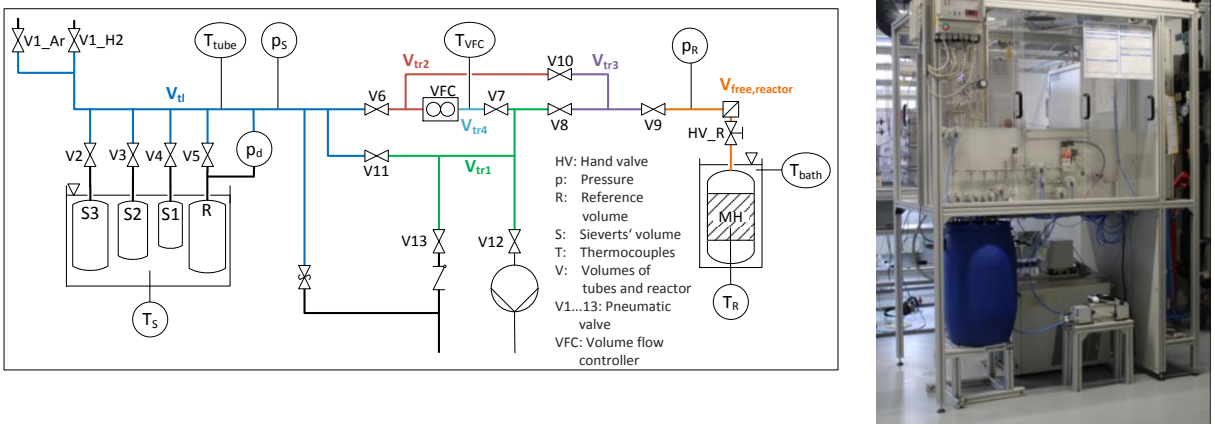

Figure 2. Layout and Picture of the characterization test bench

For near equilibrium PCI measurements, the reactor design has to allow sufficient heat and mass transfer in order to ensure reaction at constant temperature. Due to the small volume flow rates, an inner tube diameter of 9 mm satisfies this

requirement, at the same time realizing enough sample mass to generate measurement values well above the measurement precision. The temperature change inside the reactor was measured by a thermocouple type K at the center of the tube, approx. 13 mm above the lower end of the reactor. The design limited the change of temperature of the material to less than 3 K at all times for all measurements, see details in [18]. The used reactor is shown in Figure 3, left. The stainless steel tube (d_{out} = 12 mm) had a length of approx. 100 mm. A hand valve protects the material at installation. A filter with a pore size of 0.5 µm was added to prevent the powder material from moving. A sample mass of 10.63 g of $LaNi_{4.85}Al_{0.15}$ and 6.20 g of C5 has been used.

Due to the fast reaction, for the reaction rate measurements, aluminum powder with a particle diameter below 160 µm is used as thermal ballast to disperse the heat of reaction quickly. The diameter, on the one hand, is considered to be small enough to mix well with the metal hydride of a diameter of approx. 5 µm and, on the other hand, large enough for small pressure losses to allow good gas transfer ability through the bed. Additionally, relatively high pressure during the experiments of up to 20 bar further enhances the gas transport. This, however, might lead to the complete formation of the β-phase. This effect can be minimized by considering measurements only until 80 % are transformed, related to the overall conversion. Different expressions for the reaction mechanism have been calculated for the experiments and the reaction of first order was found to fit all results [18].

Two charges were investigated, both prepared the same way. The total sample mass of 21 g contained a metal hydride mass of 0.38 g of $LaNi_{4.85}Al_{0.15}$ and an aluminum mass of 20.62 g (factor of 55). The mixture was inserted into a stainless steel tube with an inner diameter of 9 mm (d_{out} = 12 mm). The temperature of the material was

measured by a thermocouple type K at a height of approx. 10 mm from the bottom. A picture of the reactor is given on the right hand side of Figure 3. This design allowed a small temperature change of below 3 K for all experiments, which is shown in the supplementary material in Figure A-1.

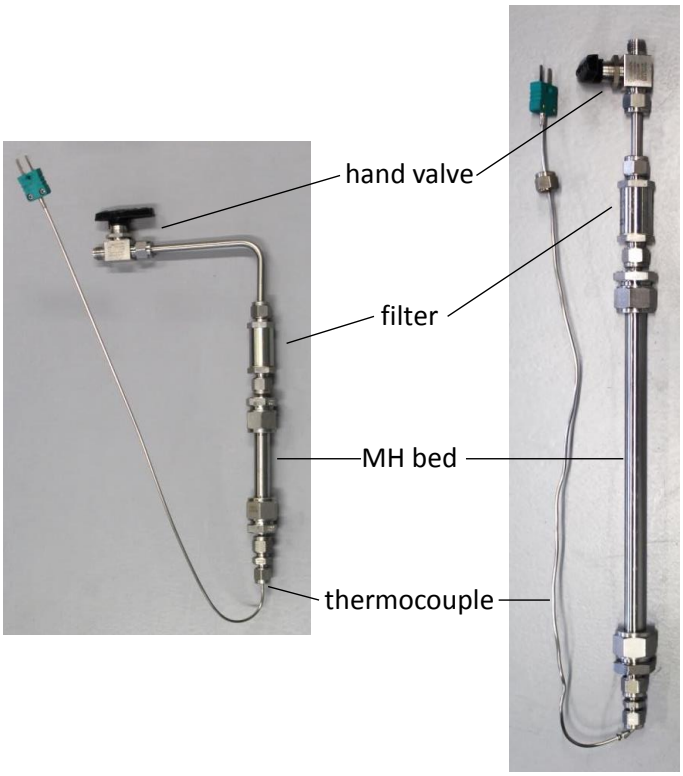

Figure 3. Reactor for dynamic pressure concentration-isotherm measurements (left) and reactor for reaction rate measurements (right)

2.3.Analysis

2.3.1. Pressure concentration-isotherm (PCI)

The value of interest for PCI measurements is the equilibrium pressure as function of hydrogen conversion and reaction temperature. The conversion of each measurement step is derived from the pressure drop in the Sieverts' volume. The yield conversion value is related to the measured equilibrium pressure in the metal hydride reactor. Due to the constant mass flow during the dynamic measurement, the

pressure change in the reactor already shows the typical shape of a PCI. An exemplary measurement result is shown in the supplementary material in Figure A-2.

For absorption, the hydrogen conversion is calculated from the pressure change in the Sieverts' volume, taking the temporal change of the temperatures in all volumes into account. Desorption is controlled and measured by the volume flow control. For balancing, the sum of its values every 0.5 s would lead to lower accuracy. However, the material has to desorb the same amount as was absorbed, because during the next absorption process, the same hydrogen conversion value was reached (without additional desorption). Therefore, the hydrogen conversion during desorption is normalized by fitting the overall released hydrogen to the value for the absorption. The ideal gas law was used, because the compressibility factor of hydrogen at the considered temperatures and pressures of below 1.03 [40] is negligible. Details on the calculations are given in the supplementary material "Analysis".

Only the plateau of the PCI is of importance when considering equilibrium properties for thermal applications, because here, the vast majority of hydrogen is converted and the pressure only changes slightly with conversion. The plateau slope m_{pl} for each PCI curve was determined by using equation (2).

$$m_{pl} = \left. \frac{d\left(\ln \frac{p_{eq}}{p_0}\right)}{d\omega} \right|_{\omega_{mid}} \quad \textbf{(2)}$$

The equilibrium states for each temperature and both absorption and desorption was determined from the PCI curves. The temperature dependent van't Hoff equation (3) can be fitted to these values resulting in values for the reaction enthalpy $\Delta_R H$ and entropy $\Delta_R S$. [14], [41]

$$\ln\left(\frac{p_{eq}}{p_0}\right) = \frac{-\Delta_R H}{R\,T} + \frac{\Delta_R S}{R} \quad \textbf{(3)}$$

For $LaNi_{4.85}Al_{0.15}$, 11 experiments were conducted in a temperature range between -20 and 130 °C and 5 experiments were conducted for C5 in a temperature between -30 and 35 °C. The experiments were designed to find the maximal hydrogen flow rate for near equilibrium approach. For the large temperature range of the experiments with $LaNi_{4.85}Al_{0.15}$, here, a flow rate at a medium temperature level was additionally determined. More details on the experiments conducted are given in detail in Table A-3 of the supplementary material.

2.3.2. Reaction rate coefficient

The measured value is the pressure drop, which correlates to the hydrogen conversion, over time. An exemplary measurement is shown in the supplementary material in Figure A-3. The correlation between the hydrogen conversion over time $\frac{\partial x}{\partial t}$ during the measurement and the desired temperature dependent rate coefficient $k(T)$ is given in equation (4). The pressure dependence function $f(p)$ is interpreted differently in literature, leading to a large discrepancy between the results, as was pointed out by Ron in [1]. As a consequence, he proposes a normalization method (normalized pressure dependence method, NPDM), allowing good comparison of different experimental set-ups. Therefore, this work follows this method with the pressure dependence function as given in equation (5). The reaction mechanism $f(x)$ has to describe the rate controlling step correctly in order to yield a correct rate coefficient. Although there is no consensus in literature on the precise hydrogenation process [18], fortunately, for fast reactions, the measurement analysis of the reaction rate allows an approximation of the correctly reflected characteristics of the pressure

dependence and mechanism functions. This can be ensured by using the ratio of their antiderivatives (cf. equation (7)). Here, all results have to coincide with one line and the slope corresponds to the rate coefficient. If this is the case, then the pressure dependence and mechanism are reflected correctly and the rate coefficient can be derived. Different expressions have been calculated for the experiments in this work and the reaction mechanism of first order as given in equation (6) [1], [42] was found to be suitable for all results. Figure A-4 of the supplementary material shows the fit of equation (7) to an exemplary experiment. With experimental results at varied temperatures, the explicit equation for the temperature dependent Arrhenius term for the rate coefficient can be derived. It is given in equation (8) and leads to the pre-exponential factor A in s^{-1} and the activation energy E_a in kJ/mol.

$$\frac{\partial x}{\partial t} = k(T) \cdot f(p) \cdot f(x) \tag{4}$$

$$f(p) = \frac{|p_{eq} - p|}{p_{eq}} \tag{5}$$

$$f(x) = 1 - x \tag{6}$$

$$\frac{F(x)}{f(p)} = \frac{-\ln(1-x) \cdot p_{eq}}{|p_{eq} - p|} = k(T) \cdot t \tag{7}$$

$$k(T) = A \exp\left(-\frac{E_a}{RT}\right) \tag{8}$$

For the calculation, the transformed fraction, the equilibrium pressure at material temperature and the pressure in the reactor over time are needed.

The following assumptions are made for the analysis:

- The temperature of the Sieverts' volume is assumed to stay constant for the whole reaction time

- Due to the very short reaction time, the hydrogen supplied from the Sieverts' volume is assumed to stay at its temperature rather than to adopt reactor temperature

The equilibrium pressure is calculated at the set temperature of the material using the results of the PCI measurements. Since the plateau slope of $LaNi_{4.85}Al_{0.15}$ is very small, it is neglected in this calculation.

With two different charges, 12 experiments were performed in total in a temperature range between -20 and 40 °C. Details are given in Table 2 in the result section.

2.4.Experimental design and repeatability

The experiments were designed in order to fit the boundary conditions of the described preheating application in vehicles and to exclude errors due to the order of experiments. Several experiments were repeated during the experimental phase to exclude changes of the material or between the different charges. The results show no effect of these considered parameters. For all experiments, accurate pressure sensors for the according pressure ranges were used.

For the PCI measurements, different hydrogen flow rates were investigated in order to identify the conditions that allow for measurements as close as possible to the equilibrium while taking the least time possible. $LaNi_{4.85}Al_{0.15}$ was investigated between -20 and 130 °C and C5 between -30 and 35 °C. Details are given in Table A-3 in the supplementary material.

For the reaction rate measurements, $LaNi_{4.85}Al_{0.15}$ was investigated in a temperature range between -20 and 40 °C. For extensive measurements, different end pressures after full conversion were investigated. They relate to different factors f between end

pressure and equilibrium pressure at the given temperature according to equation (9):

$$f = \frac{p_{end}(x_{end})}{p_{eq}(T_{MH})} \quad \textbf{(9)}$$

The investigated factors ranged between 2 and 57. For all factors, similar rate coefficients were obtained. Therefore we conclude that gas transport was sufficient for all investigated pressures. Details are given in Table 2 in the result section.

The repeatability of all experiments was excellent. For the PCI measurements, repeated experiments as well as results for different hydrogen flow rates and the chosen values are given in the supplementary material in Figure A-5. Figure A-6 shows repeated experiments for the rate coefficient measurements and their agreement.

3. Results and discussion

The aim of this work was to develop a precise experimental set-up for metal hydride characterization and to provide thermodynamic and kinetic properties for two different metal hydrides suitable for vehicle applications below 0 °C. The presented test bench is able to characterize metal hydrides in a large temperature and pressure range at high precision.

In this section, first the results of the PCI measurements are presented. Comparison to literature at the same temperature allows evaluation of the quality of the results. Then, the measurements can be extended to lower, previously not investigated

temperatures. From the obtained PCIs, the van't Hoff-plots and the values for reaction enthalpy and entropy are derived.

The reaction rate measurements for $LaNi_{4.85}Al_{0.15}$ are presented and the pre-exponential factor and the activation energy are derived. The results are compared to measurement for $LaNi_5$ from literature in order to evaluate the effect of the Al-substitution.

Finally, the obtained properties are discussed regarding the considered vehicle application.

3.1. Results on PCI measurements

In Figure 4, the PCI measurement results for both materials are compared to literature data at the respective temperature. As can be seen, there is good agreement between the data. Some deviations can be identified at the beginning of absorption and desorption, however, the largest variations occur between the different literature values for C5. Overall, all values show close agreement, in particular the level of the plateaus for both absorption and desorption agree well. Therefore, the expansion to lower temperatures and pressures promises reliable results.

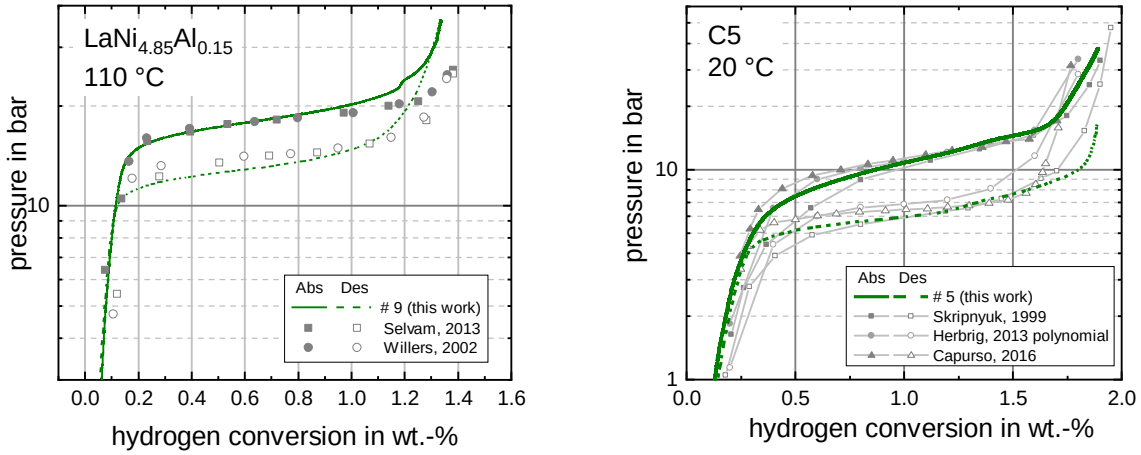

Figure 4. Comparison of results of $LaNi_{4.85}Al_{0.15}$ to literature [21], [23] **(left) and C5 to literature** [25]–[27] **(right)**

The final PCI results for both materials are given in Figure 5. To our knowledge, they represent the first publication of thermodynamic values at temperatures below 25 °C and 0 °C for $LaNi_{4.85}Al_{0.15}$ and C5, respectively. They allow precise description of the equilibrium state down to -20 °C for $LaNi_{4.85}Al_{0.15}$ and -30 °C for C5 and hence extend the available data for both absorption and desorption to lower temperatures. For details on the used experiments, refer to Table A-3 in the supplementary material. The upper part of Figure 5 shows the results for $LaNi_{4.85}Al_{0.15}$. The PCIs are given on the left hand side. The van't Hoff-plot on the right hand side is derived for 10, 50 and 90 % of hydrogen conversion for both absorption and desorption. It can be observed that the material exhibits a very small plateau slope and small hysteresis compared to other metal hydrides. At -20 °C, $LaNi_{4.85}Al_{0.15}$ shows an equilibrium pressure of 55 mbar for desorption and 120 mbar for absorption at mid-plateau.

The lower part of Figure 5 shows the results for C5. Although the experiments have been conducted with great care and possible effects of the analysis were looked at intensively (see [18]), the overall hydrogen conversion shows slightly smaller values

for decreased temperatures. This behavior does not coincide with reported general metal hydride properties, from which one would expect an increase of the plateau at lower temperatures. The reason for this deviation is unclear. However, the resulting pressure level of the α+β-phase is not affected but allows precise description of the mid-plateau. Hence, the curves were aligned at 50 % conversion and these values were used for the evaluation of the van't Hoff-plot. C5 reacts between 580 mbar for desorption and 1.6 bar for absorption at -30 °C at mid-plateau.

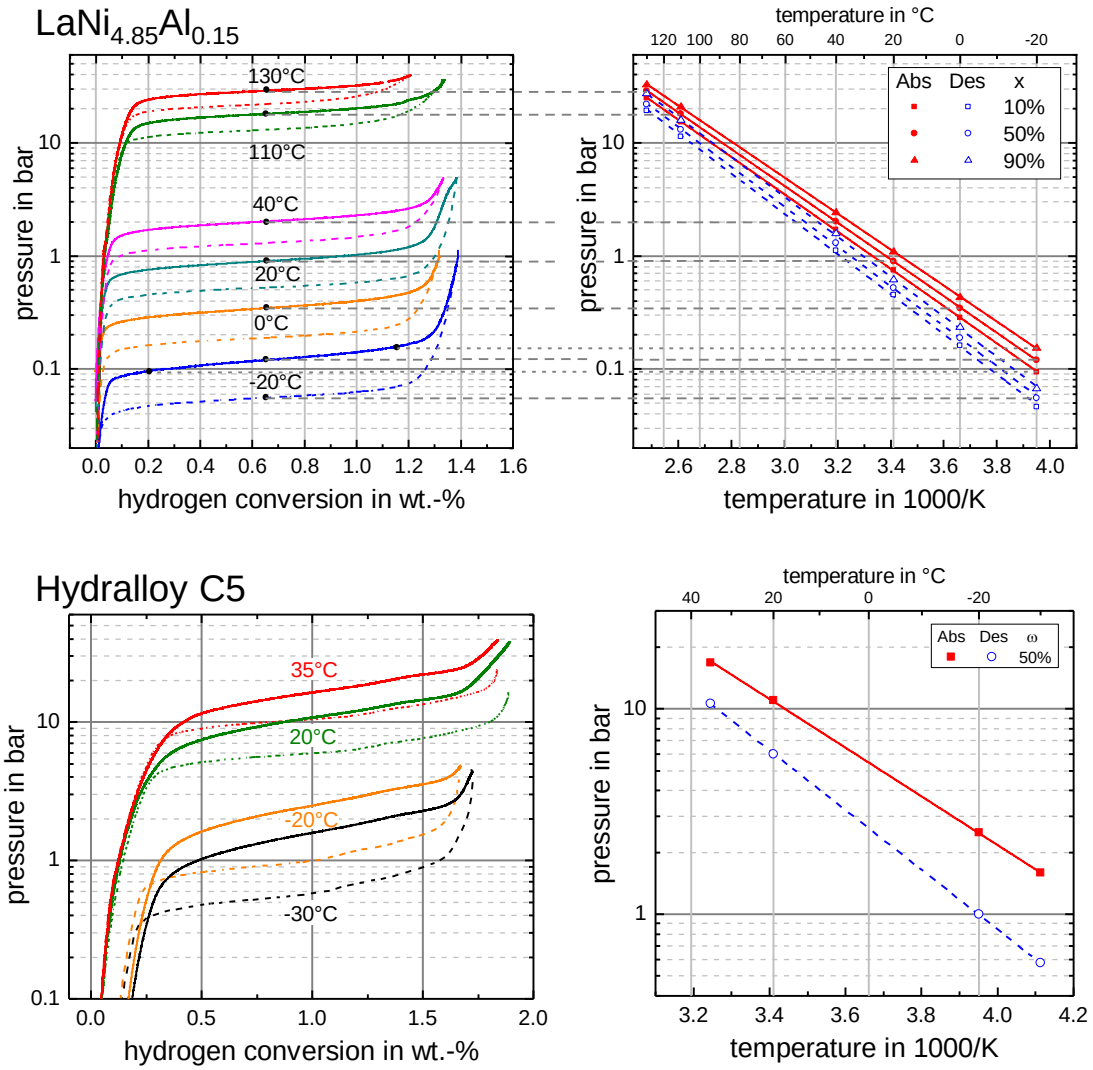

Figure 5. PCI measurements (left) and resulting Van't Hoff plot (right) for absorption (solid) and desorption (dashed) for $LaNi_{4.85}Al_{0.15}$ and for C5

From the van't Hoff-plots on the right hand side of Figure 5, the reaction enthalpy and entropy were derived. Additionally, the PCI plateau slope at the middle of the plateau ω_{mid} is deduced. The values are given in Table 1. The very small value for the plateau slope of $LaNi_{4.85}Al_{0.15}$ of 0.004 wt.-%$^{-1}$ underlines the close horizontal shape of this plateau. For C5, the slope with values between 0.53 and 0.72 wt.-%$^{-1}$ shows a considerably steeper course, which is typical for many Ti-Zr-Mn alloys.

Table 1. Reaction enthalpy, entropy and plateau slope for $LaNi_{4.85}Al_{0.15}$ and C5

$LaNi_{4.85}Al_{0.15}$							
	x in %	$\Delta_R H$ in kJ/mol	$\Delta_R H_{mean}$	$\Delta_R S$ in J/(mol K)	$\Delta_R S_{mean}$	m_{pl} in wt.-%$^{-1}$	ω_{mid} in wt.-%
absorption	10	31.54	31.0	105.05	104.9	0.004	0.65
	50	31.08		105.10			
	90	30.47		104.66			
desorption	10	33.98	33.8	109.08	109.9		
	50	33.70		109.41			
	90	33.76		111.27			
C5							
	x in %	**$\Delta_R H$ in kJ/mol**		**$\Delta_R S$ in J/(mol K)**		**m_{pl} in wt.-%$^{-1}$**	**ω_{mid} in wt.-%**
absorption	50	22.69		97.20		0.723	1.0
desorption	50	27.83		109.90		0.534	

3.2. Results on reaction rate coefficient measurements

The reaction rate of $LaNi_{4.85}Al_{0.15}$ was investigated in the range of -20 to 40 °C. The resulting reaction rate coefficient are depicted in Figure 6 and all values, together with measurement specifications, are given in Table 2. The rate coefficient values for C5 from [27] are also included in the figure. The rate coefficients for $LaNi_{4.85}Al_{0.15}$ are clearly below the values for C5. However, they still show high values compared to other metal hydrides, e.g. the reaction rate coefficient of $LaNi_{4.85}Al_{0.15}$ at -20 °C is 0.0018 s^{-1}. Hence hydrogen conversion to a value of 90 % would take around

8.5 min[b]. The reaction rate at 20 °C increases to 0.019 s^{-1}, leading to less than 1 min for complete conversion[b].

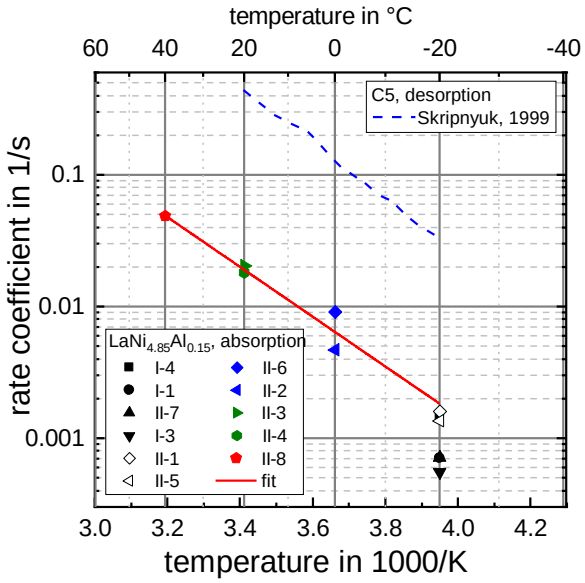

Figure 6. Rate coefficients for $LaNi_{4.85}Al_{0.15}$ for all performed experiments and for C5 [27]

Table 2. Results of all reaction rate experiments

No. of exp.	T in °C	p-sensor	p_{end} in bar	factor f	k in 1/s
I-4	-20	$p_{R,5}$	0.24	2	0.00148
I-1			0.8	7	7.08861E-4
II-7					7.16806E-4
I-3			1.5	13	5.56077E-4
II-1			4.2	35	0.00159
II-5					0.00136
II-6	0		3.5	10	0.00911
II-2		$p_{R,40}$	20	57	0.00469
I-2*	20	$p_{R,5}$	4.2	5	-
II-3					0.02057
II-4		$p_{R,40}$	20	22	0.01828
II-8	40		20	10	0.04887

* excluded due to unreasonable results

From the values for the reaction rate coefficient, the Arrhenius equation (8) can be used to derive the pre-exponential factor and the activation energy. For $LaNi_{4.85}Al_{0.15}$ the values are $A = 53{,}726\ s^{-1}$ and $E_a = 36{,}202\ \frac{\mathrm{J}}{\mathrm{mol}}$. Therefore, the resulting Arrhenius term is as follows (10):

[b] At isothermal conditions and if only the reaction rate coefficient would determine the time

$$k(T) = 5.4 \cdot 10^4 \frac{1}{s} \cdot \exp\left(\frac{-36.2 \frac{kJ}{mol}}{RT}\right) \quad \textbf{(10)}$$

The effect of the substitution of nickel by aluminum on the reaction rates is discussed controversy in literature. Although, even for the well investigates $LaNi_5$, publications don't agree on the exact rate coefficients for this material, showing the difficulty of these measurements such as isothermal conditions, a range can be defined and compared to the findings of this work for $LaNi_{4.85}Al_{0.15}$, see Figure 7. As can be seen, the slope of the line for $LaNi_{4.85}Al_{0.15}$ is similar to the literature values for $LaNi_5$, however, at a higher level. For example at 20 °C, the reaction rate of $LaNi_{4.85}Al_{0.15}$ is higher by a factor of around 2. Hence, it can be stated, at least for the investigated derivative, that the small aluminum content enhances the reaction rates.

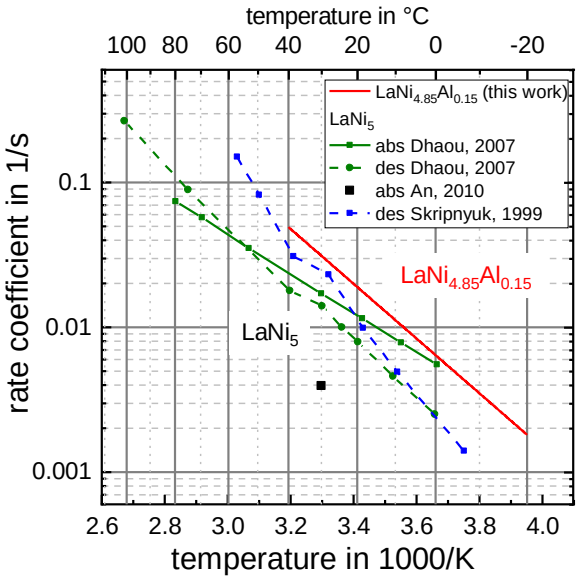

Figure 7. Rate coefficient for $LaNi_{4.85}Al_{0.15}$ compared to $LaNi_5$ [22], [27], [28]

3.3.Discussion in the context of vehicle application

In order to provide sufficient thermal energy for the vehicle component, of course much more material is required than for the characterization measurements. In order

to provide sufficient thermal energy for preheating of e.g. 1 l of engine oil (in smaller circuit for cold start), 1 kg of material has to be considered for a temperature rise of 35 K. Therefore, large scale effects such as gas or heat transport limitations will occur. Hence, the chosen pair for the closed system and the heat generating material for the open system have to allow for temperature and pressure losses as well as for non-isothermal conditions and the system still has to work.

For the closed system in an ICE vehicle, the chosen material pair shows promising characteristics in this regard. In Figure 8, the temperature boundary conditions are given together with the thermochemical equilibrium and reaction rates of the metal hydrides.

On the left hand side, the regeneration temperature level between 90 and 130 °C applied to $LaNi_{4.85}Al_{0.15}$ shows the resulting temperature level of absorption in C5 between 10 and 50 °C. According to the derived data, this absorption heat can always be released to the ambient. At elevated ambient temperatures, higher regeneration temperatures are required. This matches the experimental observation in [17], where, including temperature and pressure losses, a temperature difference between regeneration and ambient level of at least 110 K was necessary. During discharge, a theoretical temperature level between 20 to 70 °C can be reached for preheating.

Due to non-isothermal conditions, the materials will change their temperature during reaction, as indicated in Figure 8, right. For the heat generating material, this leads to a temperature increase which is beneficial for the reaction rate. A temperature increase from -20 °C by 10 K leads to an increase in the reaction rate coefficient by a factor of around 2, leading to full conversion within 5 min instead of 9 min[b]. In contrast, for the hydrogen supplying material, desorption will lead to temperature

decrease. For example, a decrease of 10 K from -20 °C leads to a decrease of the reaction rate coefficient by a factor of 2 and the time for full conversion is prolonged from half a minute to around one minute[b]. However, since this is still very fast, the temperature decrease will most likely allow for sufficiently fast reaction.

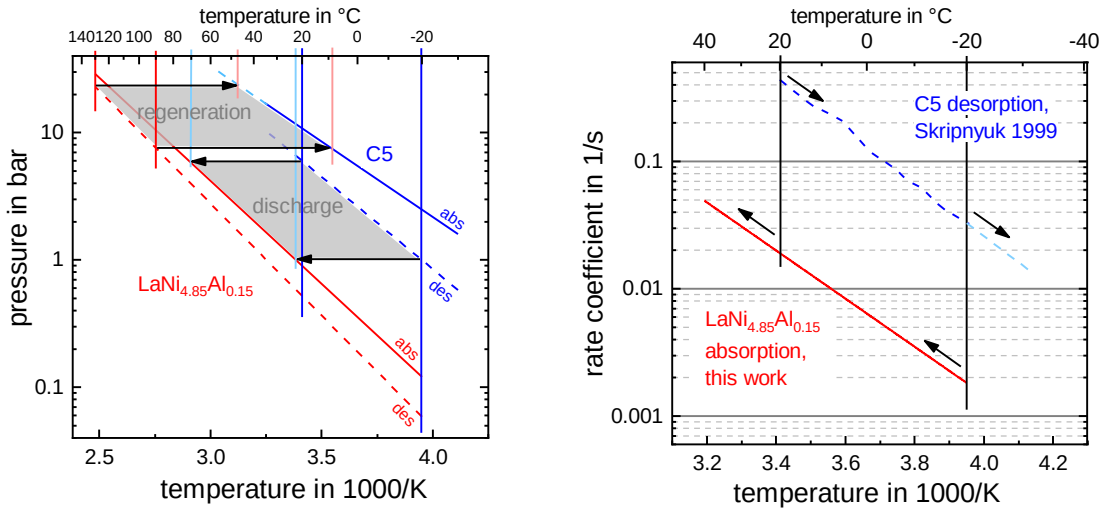

Figure 8. Material properties and vehicle boundary conditions

For the open system in a FC vehicle, the heat generating material $LaNi_{4.85}Al_{0.15}$ meets the requirements as well. Absorption at 1 bar and higher from the hydrogen storage tank leads to absorption temperature levels significantly above freezing point. Regeneration at 60 °C from FC waste heat leads to a desorption pressure above 2 bar and hence the hydrogen can be converted in the FC [17]. As for the closed system, the absorption heat also leads to a temperature increase and hence the reaction rate increases (self-acceleration). Higher pressures than in the closed system are possible and lead to even higher equilibrium temperatures and reaction rates.

Therefore, the material properties satisfy the vehicle requirements at the considered boundary conditions. However, in particular for the closed system, scale up effects

might require higher temperature differences than suggest by the intrinsic material properties (PCI) and non-isothermal conditions might lead to limitations in extreme cases.

4. Conclusion

Almost no data is known in literature about equilibrium pressures and reaction rates of metal hydrides below 0 °C. However, for thermal applications in vehicles operated in winter conditions, this knowledge is crucial. This work presents a precise experimental set-up to measure characteristics of metal hydrides in the temperature range of -30 to 200 °C and a pressure range of 0.1 mbar to 100 bar. Pressure concentration-isotherms for $LaNi_{4.85}Al_{0.15}$ and C5 ($Ti_{0.95}Zr_{0.05}Mn_{1.46}V_{0.45}Fe_{0.09}$) and reaction rate coefficients for $LaNi_{4.85}Al_{0.15}$ were measured in the temperature and pressure range necessary for vehicle preheating applications.

The first PCIs for both materials below 0 °C were published here. For $LaNi_{4.85}Al_{0.15}$, reaction rate coefficients down to -20 °C were measured for the first time and compared to values of $LaNi_5$ for the effect of nickel-substitution by aluminum. Only now, the characteristics of the material can be described in the necessary range for vehicle applications. $LaNi_{4.85}Al_{0.15}$ shows an equilibrium pressure down to 55 mbar for desorption and 120 mbar for absorption at mid-plateau at -20 °C. C5 reacts between 580 mbar for desorption and 1.6 bar for absorption at -30 °C at mid-plateau.

Beneficial for the application, the rate coefficient results for $LaNi_{4.85}Al_{0.15}$ show high values even at -20 °C of 0.0018 s^{-1}. Compared to $LaNi_5$, the aluminum addition in $LaNi_{4.85}Al_{0.15}$ leads to increased reaction rates. C5 shows even higher values, namely by a factor of more than 10 even at -20 °C.

However, in vehicle applications a sufficient amount of heat needs to be stored. This required increase in mass of material will lead to gas and heat transport limitations. Hence, experiments in large scale have to show the up-scale limitation factors of the material pair in the considered applications. First measurements have been performed by the authors and published in [17]. Together with the complementary data presented here, preheating units that reduce automotive cold-start issues can be developed.

References

[1] M. Ron, "The normalized pressure dependence method for the evaluation of kinetic rates of metal hydride formation/decomposition," *J. Alloys Compd.*, vol. 283, no. 1–2, pp. 178–191, 1999.

[2] R. Cipollone, D. Di Battista, and M. Mauriello, "Effects of oil warm up acceleration on the fuel consumption of reciprocating internal combustion engines," *Energy Procedia*, vol. 82, pp. 1–8, 2015.

[3] M. S. Reiter and K. M. Kockelman, "The problem of cold starts: A closer look at mobile source emissions levels," *Transp. Res. Part D Transp. Environ.*, vol. 43, pp. 123–132, 2016.

[4] D. Di Battista and R. Cipollone, "Experimental and numerical assessment of methods to reduce warm up time of engine lubricant oil," *Appl. Energy*, vol. 162, pp. 570–580, 2016.

[5] D.-W. Lee, J. Johnson, J. Lv, K. Novak, and J. Zeitsman, "Comparisons between vehicular emissions from real-world in-use testing and epa moves estimation," 2012.

[6] D. K. Deppenkemper, M. Günther, and P. Stefan, "Development of optimized exhaust gas heating strategies for passenger car Diesel engines by means of variable valve train applications," in *17. Internationales Stuttgarter Symposium*, 2017, pp. 123–142.

[7] C. Dardiotis, G. Martini, A. Marotta, and U. Manfredi, "Low-temperature cold-start gaseous emissions of late technology passenger cars," *Appl. Energy*, vol. 111, pp. 468–478, 2013.

[8] Q. Fan and L. Li, "Study on first-cycle combustion and emissions during cold start in a TSDI gasoline engine," *Fuel*, vol. 103, pp. 473–479, 2013.

[9] S. Q. A. Rizvi, *A Comprehensive Review of Lubricant Chemistry , Technology, Selection,*

and Design. West Conshohocken, PA: ASTM International, 2009.

[10] J. Mishler, Y. Wang, P. P. Mukherjee, R. Mukundan, and R. L. Borup, "Subfreezing operation of polymer electrolyte fuel cells: Ice formation and cell performance loss," *Electrochim. Acta*, vol. 65, pp. 127–133, 2012.

[11] A. Santamaria, H. Y. Tang, J. W. Park, G. G. Park, and Y. J. Sohn, "3D neutron tomography of a polymer electrolyte membrane fuel cell under sub-zero conditions," *Int. J. Hydrogen Energy*, vol. 37, no. 14, pp. 10836–10843, 2012.

[12] S. J. Lim *et al.*, "Investigation of freeze/thaw durability in polymer electrolyte fuel cells," *Int. J. Hydrogen Energy*, vol. 35, no. 23, pp. 13111–13117, 2010.

[13] R. Lin, X. Lin, Y. Weng, and Y. Ren, "Evolution of thermal drifting during and after cold start of proton exchange membrane fuel cell by segmented cell technology," *Int. J. Hydrogen Energy*, vol. 40, no. 23, pp. 7370–7381, 2015.

[14] M. Dornheim, "Thermodynamics of metal hydrides: Tailoring reaction enthalpies of hydrogen storage materials," in *Thermodynamics - Interaction Studies - Solids, Liquids and Gases*, Dr. Juan Carlos Moreno Pirajan, Ed. Intech open science - open minds, 2011.

[15] J. Bloch and M. H. Mintz, "Kinetics and mechanisms of metal hydrides formation—a review," *J. Alloys Compd.*, vol. 253–254, pp. 529–541, 1997.

[16] P. Muthukumar, A. Satheesh, M. Linder, R. Mertz, and M. Groll, "Studies on hydriding kinetics of some La-based metal hydride alloys," *Int. J. Hydrogen Energy*, vol. 34, no. 17, pp. 7253–7262, 2009.

[17] M. Dieterich, I. Bürger, and M. Linder, "Open and closed metal hydride system for high thermal power applications: Preheating vehicle components," *Int. J. Hydrogen Energy*, vol. 42, no. 16, pp. 11469–11481, 2017.

[18] M. Kölbig, "Coupled metal hydride reactions for preheating vehicle components at low temperatures," University of Stuttgart, 2018.

[19] C. Weckerle, I. Buerger, and M. Linder, "Novel reactor design for metal hydride cooling systems," *Int. J. Hydrogen Energy*, vol. 42, no. 12, pp. 8063–8074, 2017.

[20] N. Mechi, I. Ben Khemis, H. Dhaou, S. Knani, A. Jemni, and A. Ben Lamine, "A macroscopic investigation to interpret the absorption and desorption of hydrogen in LaNi4.85Al0.15 alloy using the grand canonical ensemble," *Fluid Phase Equilib.*, vol. 427, pp. 56–71, 2016.

[21] P. K. Selvam, P. Muthukumar, M. Linder, R. Mertz, and R. Kulenovic, "Measurement of thermochemical properties of some metal hydrides – Titanium (Ti), misch metal (Mm) and lanthanum (La) based alloys," *Int. J. Hydrogen Energy*, vol. 38, no. 13, pp. 5288–5301, 2013.

[22] H. Dhaou, F. Askri, M. Ben Salah, A. Jemni, S. Ben Nasrallah, and J. Lamloumi, "Measurement and modelling of kinetics of hydrogen sorption by LaNi5 and two related pseudobinary compounds," *Int. J. Hydrogen Energy*, vol. 32, no. 5, pp. 576–

587, 2007.

[23] E. Willers, “Multi-Hydrid-Sorptionsanlage zur kombinierten Heizung und Kühlung,” University of Stuttgart, 2002.

[24] M. Wanner, “Untersuchung des Langzeitverhaltens der thermodynamischen Stabilität von Metallhydriden,” University of Stuttgart, 2001.

[25] G. Capurso *et al.*, “Development of a modular room-temperature hydride storage system for vehicular applications,” *Appl. Phys. A*, vol. 122, no. 3, p. 236, 2016.

[26] K. Herbrig, L. Röntzsch, C. Pohlmann, T. Weißgärber, and B. Kieback, “Hydrogen storage systems based on hydride–graphite composites: computer simulation and experimental validation,” *Int. J. Hydrogen Energy*, vol. 38, no. 17, pp. 7026–7036, 2013.

[27] V. M. Skripnyuk and M. Ron, “Evaluation of kinetics by utilizating the mormalized pressure dependence method for the alloy Ti0.95 Zr0.05 Mn1.48 V0.43 Fe0.08 Al0.01,” *J. Alloys Compd.*, vol. 295, pp. 385–390, 1999.

[28] X. H. An, Y. B. Pan, Q. Luo, X. Zhang, J. Y. Zhang, and Q. Li, “Application of a new kinetic model for the hydriding kinetic of LaNi5-xAlx ($0 \leq x \leq 1.0$) alloys,” *J. Alloys Compd.*, vol. 506, no. 1, pp. 63–69, 2010.

[29] V. K. Sharma and E. Anil Kumar, “Measurement and analysis of reaction kinetics of La – based hydride pairs suitable for metal hydride – based cooling systems,” *Int. J. Hydrogen Energy*, vol. 39, no. 33, pp. 19156–19168, 2014.

[30] D. L. Cao, H. H. Cheng, L. Ma, D. M. Chen, M. Q. Lue, and K. Yang, “Effects of Al partial substitution for Ni on properties of LaNi5-xAlx,” *Trans. Nonferrous Met. Soc. China*, vol. 17, no. 50276063, pp. S967–S971, 2007.

[31] X.-L. Wang and S. Suda, “Effects of Al-substitution on hydriding reaction rates of LaNi5-xAlx,” *J. Alloys Compd.*, vol. 191, no. 1, pp. 5–7, 1993.

[32] I.-S. Park, J.-K. Kim, K. J. Kim, J. Zhang, C. Park, and K. Gawlik, “Investigation of coupled AB5 type high-power metal hydride reactors,” *Int. J. Hydrogen Energy*, vol. 34, no. 14, pp. 5770–5777, 2009.

[33] A. J. Goudy, D. G. Stokes, and J. A. Gazzillo, “The effect of heat transfer on the desorption kinetics of LaNi5H6,” *J. Less Common Met.*, vol. 91, no. 1, pp. 149–158, 1983.

[34] X.-L. Wang and S. Suda, “Study of the hydriding kinetics of LaNi4.7Al0.3-H system by a step-wise method,” *J. Less Common Met.*, vol. 159, pp. 109–119, 1990.

[35] F. Feng, M. Geng, and D. O. Northwood, “Mathematical model for the plateau region of P–C-isotherms of hydrogen-absorbing alloys using hydrogen reaction kinetics,” *Comput. Mater. Sci.*, vol. 23, no. 1–4, pp. 291–299, 2002.

[36] G. Friedlmeier, M. Schaaf, and M. Groll, “How to measure pressure-concentration-isotherms representative for technical applications,” *Zeitschrift für Phys. Chemie*, vol.

183, pp. 185–195, 1994.

[37] P. Muthukumar, M. Linder, R. Mertz, and E. Laurien, “Measurement of thermodynamic properties of some hydrogen absorbing alloys,” *Int. J. Hydrogen Energy*, vol. 34, no. 4, pp. 1873–1879, 2009.

[38] P. D. Goodell and P. S. Rudman, “Hydriding and dehydriding rates of the LaNi5-H system,” *J. Less Common Met.*, vol. 89, no. 1, pp. 117–125, 1983.

[39] P. S. Rudman, “Hydriding and dehydriding kinetics,” *J. Less-Common Met.*, vol. 89, no. 1, pp. 93–110, 1983.

[40] L. Zhou and Y. Zhou, “Determination of compressibility factor and fugacity coefficient of hydrogen in studies of adsorptive storage,” *Int. J. Hydrogen Energy*, vol. 26, no. 6, pp. 597–601, 2001.

[41] J. Huot, *Handbook of hydrogen storage*. Weinheim: Wiley-VCH, 2010.

[42] R. B. Jordan, *Reaction mechanisms of inorganic and organiometallic systems*. Oxford: University Press, 1998.